Experimental Investigation of Non-Line-of-Sight Channels in an Intra-Body Network at 2.38 GHz

Yomna El-Saboni
Centre for Wireless Innovation
Queen's University Belfast
Belfast, UK
yelsaboni01@qub.ac.uk

Dmitry E. Zelenchuk
Centre for Wireless Innovation
Queen's University Belfast
Belfast, UK
d.zelenchuk@qub.ac.uk

Gareth A. Conway
Centre for Wireless Innovation
Queen's University Belfast
Belfast, UK
g.conway@qub.ac.uk

William G. Scanlon
Tyndall National Institute
University College Cork
Cork, Ireland
w.scanlon@ieee.org

***Abstract*—The characteristics of the intra-body propagation channel between implanted antennas are highly application dependent. Measurements of the forward path gain between identical implant antennas within two multi-layered tissue mimicking liquid phantoms were used to investigate the nature of the intra-body channel at 2.38 GHz. One of the antennas was held in fixed locations in the phantoms and a robotic positioner with millimeter accuracy was used to vary the second antenna's position. The results show that the shortest line-of-sight path is not always dominant and depending on the particular geometry of material layers and their dielectric properties other propagation paths may also be important. This highlights the importance of careful system design in intra-body networks as the link budget between implanted nodes may need to consider alternative propagating paths, depending on the application scenario.**

***Index Terms*—implant, antenna, propagation, biomedical, intra-body network**

I. Introduction

Communication between several implantable medical devices could facilitate a wide range of medical applications, enhancing minimally invasive healthcare and long term treatments through, for instance, physiological monitoring of transplanted organs or the control of smart limbs or prosthetics [1], [2]. Within such an Intra-Body Network (IBN) the path between the nodes may be physically short but it is envisaged that some applications will require communication over longer distances and through several tissue layers that may exhibit distinctly varying dielectric properties. Examples include the control of urination through neurostimulation in the urinary bladder or muscle control in spinal injuries or chronic arthritis [3]. Therefore, it is imperative to understand the characteristics of the intra-body channel and establish how signal transmission is affected by node positioning inside the body and the nature of the surrounding tissue structures. While a small number of intra-body numerical studies have appeared in the literature, there needs to be empirical validation of the results. In this paper we utilize a semi-automated mechanical positioner to measure and empirically evaluate the link between two identical insulated antennas embedded within a multi-layered cylindrical tissue mimicking phantom and investigate the effect of varying the direct tissue properties surrounding an antenna on the channel gain.

II. Measurement of the Intra-Body Channel

Empirical evaluation of implant to implant channels in non-homogeneous scenarios is mechanically challenging and requires sophisticated multi-layered phantoms. Therefore, most studies involving IBN channels have only utilized numerical modelling techniques [4], [5], but they have clearly demonstrated how the direct path is not necessarily dominant and that this varies notably from one application to the other according to operating frequency and antenna positioning.

A. Tissue Mimicking Phantoms

Two different phantom setups were used in this study. Concentric cylindrical glass containers of 400 mm height were used to form skin-fat-muscle layered phantoms. The same outer cylinder is used in both setups (244 mm inner diameter, 2 mm thickness) and is wrapped by a double layer of solid skin-mimicking material, 2 mm thick. The material is described in [6]. The difference between the two phantoms is the diameter of the inner glass cylinder. In *Phantom 1*, the inner container had an inner diameter of 184 mm and 3 mm glass thickness while in *Phantom 2*, the inner container had an inner diameter of 141 mm (3 mm thickness), as illustrated in Fig. 1. The long cylindrical form factor of the layered phantom ensures that the dominating wave propagation from the antenna-phantom system is radial and antenna feed cable radiation effects are minimized [7].

The two cylinder approach allows for liquid muscle and fat tissue mimicking regions and the skin layer helps investigate a more realistic scenario where there is a high loss dielectric boundary between fat and air. The muscle equivalent material is described in [7] and the fat equivalent liquid used was diethylene glycol dibutyl ether [8]. The phantom materials were a very good match for the target dielectric parameters in [9] at 2.38 GHz (Table I). The phantom shape, size and tissue order is not intended to mimic a specific body region but is designed to demonstrate and highlight intra-body propagation effects. In particular, the fat and muscle tissue mimicking liquids have distinctly different dielectric properties, helping to illustrate the change in wave propagation more clearly.

TABLE I
TARGET [9] AND MEASURED TISSUE PROPERTIES AT 2.38 GHZ

Tissue Type	Relative Permittivity ϵ_r	Conductivity σ Sm^{-1}	Measured Relative Permittivity ϵ_r	Measured Conductivity σ Sm^{-1}
Muscle	52.8	1.69	54.6	1.64
Fat	5.3	0.10	5.5	0.10
Skin	38.1	1.43	32.1	1.49

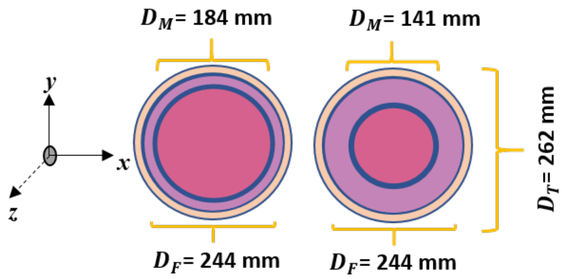

Fig. 1. Schematics of *Phantom 1* (left) and *Phantom 2* (right).

B. Antennas

Insulated printed folded meandered dipole (PFMD) antennas were used in this work due to their compact size and robustness across different tissue types without re-tuning [6]. The antennas were always fully immersed inside the tissue equivalent liquid at exactly the center of the phantom's vertical height (150 mm). The glass containers were always filled with the tissue mimicking liquid to 300 mm of height to make sure the vertical distance from the center to top or bottom of the phantom liquid is always more than the horizontal distance to outside the phantom. Both antennas (fixed and under test) were held by a 300 mm long u.fl pigtail connected to a R&S ZVB8 vector network analyser, calibrated to the feed point of each antenna.

C. Robotic Positioner

A robotic positioner was used to accurately control the movement of one of the antennas across the liquids inside the phantoms. The second (fixed) antenna was placed at four discrete fixed positions along the x-axis (x = 30, 50, 80, 110 mm), where the red line in Fig. 2 illustrates the scan path of the first antenna. The overall setup is illustrated in Fig. 3 and the antennas were attached to a rigid plastic rod to make sure they were oriented correctly.

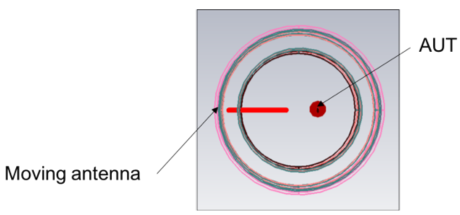

Fig. 2. Positioning of the antennas during measurements.

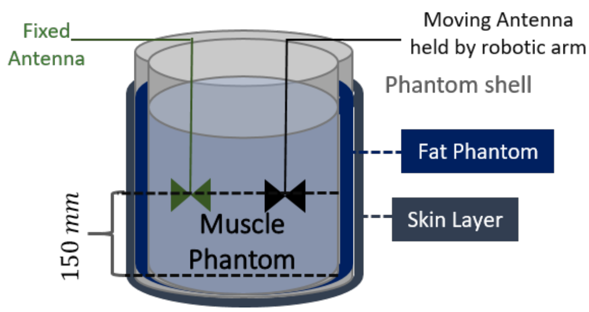

Fig. 3. Illustration of experimental setup showing tissue layers.

III. RESULTS

The IBN channel was evaluated by measuring the forward path gain $|S_{21}|$ as one antenna scans away from the second fixed antenna along the x-axis and the results are presented in Figs. 4 and 5 for *Phantom 1* and *Phantom 2*, respectively. Four different fixed positions for the second antenna (AUT) were considered and the scanned antenna was positioned at 1 mm intervals. The gap in the graphs is due to the limitation of the robotic arm, as it approaches the glass boundary in the phantoms. The results to the right of the gap are for cases when the scanned antenna is in the fat region ($x \geq 98$ mm for *Phantom 1*, $x \geq 79$ mm for *Phantom 2*).

The measurement results clearly show that the direct line-of-sight (LOS) path is not always dominant. In particular, this occurs for the the cases when both antennas are in the fat region which is either when the AUT is at 110 mm in both phantoms or the AUT is at 80 mm in *Phantom 2* and the scanned antenna is in the fat region. In both phantoms, when the fixed antenna is at 110 mm (in the fat region) the LOS distance between the antennas has less effect on forward path gain. The effect of the thicker fat layer in *Phantom 2* is also seen in the last two fixed antenna positions (80, 110) (Fig. 5) as they exhibit similar behavior.

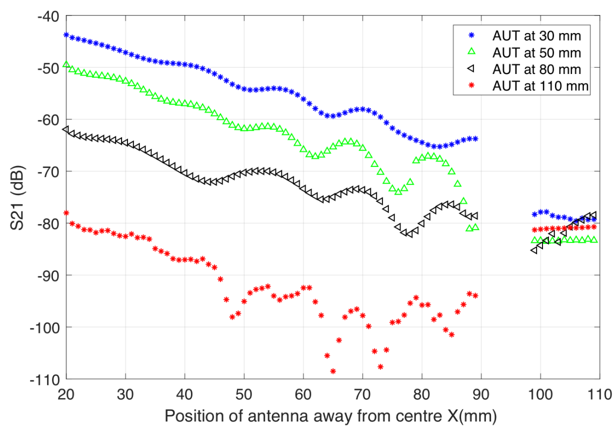

Fig. 4. Measured forward path gain $|S_{21}|$ in *Phantom 1*.

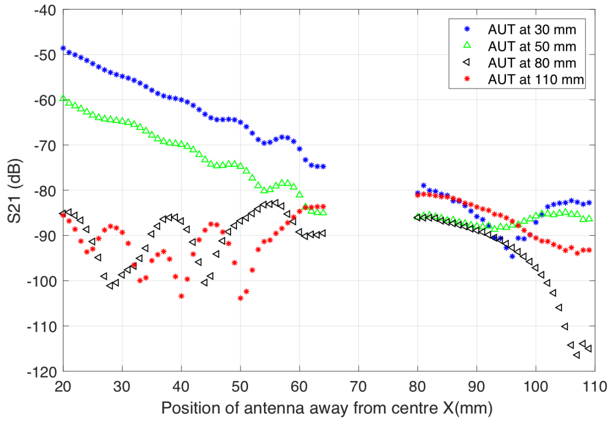

Fig. 5. Measured forward path gain $|S_{21}|$ in *Phantom 2*.

IV. Conclusion

This study validates earlier numerical studies of implant to implant intra-body channels where the lower-loss fat layer plays an important role in supporting the link between devices in the human body. The measured forward path gain results are strongly dependent on positioning and the phantom structure. Some of the phenomena observed is related to the geometrical structure of the phantom used, but the results are consistent in terms of the importance of low-loss paths being an important mechanism in IBNs. However, measurement studies of this type are notoriously difficult. In this case, as the fixed antenna was adjusted manually there is the possibility of some positional errors, although in future studies this could be mitigated through the use of a second robotic positioner.

References

[1] P. Leelatien, K. Ito, K. Saito, M. Sharma, & A. Alomainy, "Channel characteristics and wireless telemetry performance of transplanted organ monitoring system using ultrawideband communication," IEEE J. Electromagn. RF Microw. Med. Biol., vol. 2, 2, pp. 94–101, Jun. 2018.

[2] Z.Y. Chen, Y.M. Gao, & M. Du, "Propagation characteristics of electromagnetic wave on multiple tissue interfaces in wireless deep implant communication," IET Microwaves, Antennas Propag., vol. 12, 13, pp. 2034–2040, Oct. 2018.

[3] J. Massachi, Y.-K. Lo, P.-M. Wang, and W. Liu, "A wireless platform to support pre-clinical trial of neural implant for spinal cord injury," 40th Ann. Intl. Conf. IEEE Eng. Medicine & Biology Soc. (EMBC), 2018, pp. 5487–5490.

[4] Y. El-Saboni, G.A. Conway, S.L. Cotton & W.G. Scanlon, "Radiowave propagation characteristics of the intra-body channel at 2.38 GHz," 14th Intl. Conf. Wearable & Implantable Body Sensor Networks (BSN), 2017, pp. 149–152.

[5] Y. El-Saboni, G.A. Conway & W.G. Scanlon, "Effect of tissue boundaries on the intra-body communication channel at 2.38 GHz," Intl. Workshop on Antenna Technology (iWAT), 2017.

[6] M.K. Magill, G.A. Conway & W.G. Scanlon, "Tissue-independent implantable antenna for in-body communications at 2.36–2.5 GHz," IEEE Trans. Antennas Propag., vol. 65, 9, pp. 4406–4417, Sep. 2017.

[7] Y. El-Saboni, M.K. Magill, G.A. Conway, S.L. Cotton & W.G. Scanlon, "Measurement of deep tissue implanted antenna efficiency using a reverberation chamber," IEEE J. Electromagn. RF Microwaves Med. Biol., vol. 1, no. 2, pp. 90–97, Dec. 2017.

[8] "Diethylene glycol dibutyl ether, 99+%, pure, ACROS OrganicsTM 1L; Glass bottle Diethylene glycol dibutyl ether, 99+%, pure, ACROS OrganicsTM." [Online]. Available: https://www.fishersci.co.uk/shop/products/diethylene-glycol-dibutyl-ether-99-pure-acros-organics-4/10103880. [Accessed: 26-Nov-2018].

[9] S. Gabriel and R.W. Lau, "The dielectric properties of biological tissues: II. Measurements in the frequency range 10 Hz to 20 GHz," Phys. Med. Biol., vol. 41, no. 11, pp. 2251–2269, Nov. 1996.